Optimal Industrial Load Control in Smart Grid

Armen Gholian, *Student Member, IEEE,* Hamed Mohsenian-Rad,
Senior Member, IEEE, and Yingbo Hua, *Fellow, IEEE*

***Abstract*—In this paper, we investigate optimal load control in industrial sector which involves several new and distinct research problems. For example, while most residential appliances operate independently, industrial units are highly inter-dependent and must follow certain operational sequences. Also, unlike residential appliances, the operation of industrial units may span across multiple days and involve multiple batch cycles. Furthermore, in industries with process control, energy management is often coupled with material flow management. The design in this paper is comprehensive and addresses industrial load control under various smart electricity pricing scenarios, including day-ahead pricing, time-of-use pricing, peak pricing, inclining block rates, and critical peak pricing. The use of behind-the-meter renewable generator and energy storage is also considered. The formulated optimization problem is a tractable mixed-integer linear program. Different case studies are presented based on a practical energy-extensive steel mill industry model.**

***Keywords*–Demand side management, industrial load control, smart pricing, batch processes, optimal energy scheduling.**

NOMENCLATURE

$\mathcal{T}$, t	Set and index of time slots.
T	Load scheduling horizon.
$\mathcal{V}$, i	Set and index of industrial units.
$\mathcal{K}$, k	Set and index of materials.
$\mathcal{R}$, r	Set and index of initial/raw materials, $\mathcal{R} \subset \mathcal{K}$.
$\mathcal{F}$, f	Set and index of final materials/products, $\mathcal{F} \subset \mathcal{K}$.
a_i	Number of time slots in each cycle of unit i.
$s_i[t]$	Number of unit i's batch cycles started up to time t.
$e_i[t]$	Number of unit i's batch cycles finished up to time t.
$x_i[t]$	Indicating whether unit i operates at time slot t.
$u_i[t]$	Total material that is fed to unit i at time t.
$y_i[t]$	Total material that is produced by unit i at time t.
α_i	Minimum material capacity of unit i.
β_i	Maximum material capacity of unit i.
$m_k[t]$	Amount of material k available at storage at time t.
η_k	Capacity of storage for material k.
ϕ_f	Minimum amount of final product f that is needed.
$m_k[0]$	Initial amount of material k available in storage.
$M_i[t]$	Total amount of all materials inside unit i at time t.
$\mathcal{I}_k^{in}$	Set of units that use material k as an input.
$\mathcal{I}_k^{out}$	Set of units that produce material k as an output.
$\mathcal{X}$	Set of some units that must operate exclusively.
r_i^k	Required fraction of material k at the input of unit i.
q_i^k	Fraction of material k at the output of unit i.
$\mathcal{I}_{unt}$	Set of uninterruptible units.
$\mathcal{K}_{imd}$	Set of non-storable materials.
$l_i[t]$	Electricity consumption of unit i at time slot t.
c_i, d_i	Parameters of electricity consumption of unit i.
l_i^{min}	Minimum stand-by electricity consumption of unit i.
$l_{back}[t]$	Background load at time slot t.
$L[t]$	Total electricity consumption of complex at time t.
L_{max}	Power draw limit of the industrial complex.
$p[t]$	Price of electricity at time slot t.
p_f	Unit price of final product f.
p_r	Unit price of initial/raw material r.
γ_k	Cost of storing a unit of material k for one time slot.
C_{elct}	Electricity cost during scheduling horizon.
C_{fixed}	Fixed cost of the industrial complex.
$b[t]$	Indicating status of the battery system at time t.
$l_{ch}[t]$	Charge amount of the battery system at time t.
$l_{dch}[t]$	Discharge amount of the battery system at time t.
l_{ch}^{max}	Maximum charge rate of the battery system.
l_{dch}^{max}	Maximum discharge rate of the battery system.
μ	Efficiency of the battery system during charge.
θ	Efficiency of the battery system during discharge.
B^{init}	Initial charge levels of the battery system.
B^{full}	Capacity of the battery system.
$l_{slr}[t]$	Expected value of available solar energy at time t.
Ω	A large enough number.

The authors are with the Department of Electrical and Computer Engineering, University of California, Riverside, CA, 92521, USA, e-mails: armen.gholian@email.ucr.edu and {hamed, yhua}@ece.ucr.edu. The corresponding author is H. Mohsenian-Rad. This work is supported in part by NSF grant ECCS 1253516 and a GAANN Fellowship.

I. INTRODUCTION

To assure reliable service, electricity generation capacity is often designed to match the *peak demand*. Accordingly, it is desirable to minimize the peak-to-average ratio (PAR) in the aggregated demand profile in order to achieve efficient operation and to minimize the need to build new power plants. This can be done by a combination of *smart pricing* by utility companies and *optimal load control* by consumers. While the former has been widely studied in the demand response (DR) literature, e.g. [1]–[6], the latter is also of critical importance, where the focus is on exploiting the *controllable load* potential in each load sector in response to changes in price signals.

Most prior studies on optimal load control are concerned with residential [5], [7]–[12] and commercial [13]–[15] loads. However, since the industrial sector comprises 42% of the world's electricity consumption [16], addressing industrial load control (ILC) is also critical. Interestingly, since many industries are already automated, one can benefit from these existing automation infrastructures and upgrade them with control mechanisms that take into consideration power usage and demand response. Table I shows some factors that make industrial load control different from residential load control.

In this paper, an *industry* is defined as a collection of several industrial units or processes. An industrial process is either *batch* or *continuous*. In a batch process, the input materials are fed into a unit at the beginning of each batch processing cycle. The processed material are then collected at the end of

TABLE I
INDUSTRIAL VS. RESIDENTIAL LOAD CONTROL

Design Factor	Residential	Industrial
Peak Load Shaving	✓	✓
Time-Shiftable Load	✓	✓
Interruptible Load	✓	✓
Uninterruptible Load	✓	✓
Pricing Tariffs	✓	✓
On-site Renewable Generation	✓	✓
On-site Energy Storage	✓	✓
Sequential Operation		✓
Load Dependency		✓
Size of Batch Cycles		✓
Number of Batch Cycles		✓
Material Flow		✓
Material Balance		✓
Material Storage		✓
Final Products		✓
By-products		✓
Human Comfort	✓	

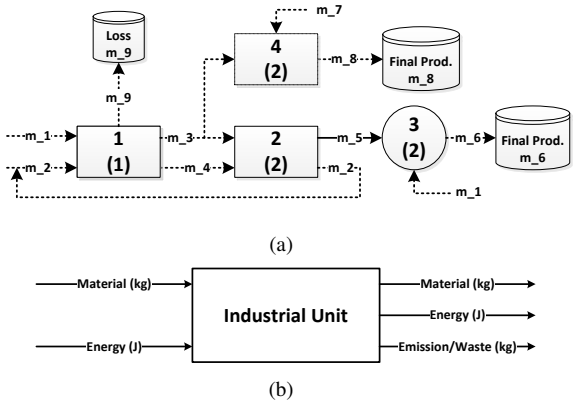

Fig. 1. An *industry* is modeled as a collection of interacting industrial units: (a) An example industry with four units and two final products. (b) Each unit is identified by its material and energy inputs and outputs, its emission and waste, and its internal operation details, e.g., whether it is interruptible.

the batch processing cycle. In contrast, in a continuous process, materials are fed and/or products are produced continuously [17]. For example, steel-making is a batch process while oil refining is mostly a continuous process. In this paper, the power usage for continuous processes is considered as uncontrollable background load while power usage for batch processes is considered as potential *controllable load*.

The contributions in this paper are summarized as follows:

- We take several industrial load details into consideration, including those that do not appear in residential or commercial load control problems. For example, industrial units are highly inter-dependent and must follow a certain operational sequence. The operation of certain industrial units may also span across multiple days. Furthermore, in industries that involve process control, energy management is often coupled with material flow management.
- Operation under different smart pricing scenarios are considered, including day-ahead pricing, time-of-use pricing, peak pricing, inclining block rates, and critical peak pricing. The uses of behind-the-meter renewable generation and energy storage are also taken into consideration.
- The formulated industrial load control optimization problem is a tractable mixed-integer linear program.
- Different case studies are presented based on a practical scenario based on a *steel mill industry* model.

This study can be compared, e.g., with [16], [18]–[22]. In [18], the benefits and challenges in ILC-based demand response are discussed; however, no specific design formulation is presented. An algorithm for ILC is proposed in [19]; however, some important industrial load features, such as the operational interdependency across industrial units are not formulated. Such details are partly discussed in [20]–[22]; however, neither [19] nor [20]–[22] considers size and the number of batch processing cycles in their formulations and whether each industrial unit is interruptible or uninterruptible. Furthermore, these studies do not take into consideration the emerging smart grid components, such as different smart pricing tariffs and the use of local renewable generation and energy storage. Finally, compared to our previous work in [16], this paper has four advantages. First, here, we manage both energy usage and material flow. Second, here, we incorporate a wider range of smart pricing models and also address local renewable generators and energy storage. Third, the system model in [16] is inherently limited to a single batch cycle. Therefore, a completely new model is used in this paper to select size and number of batch processing cycles and accordingly to conduct optimal ILC over multi-day operation horizons. Fourth, the practical steel mill industry model in this paper is also completely new and it was not discussed in [16].

II. INDUSTRIAL LOAD SYSTEM MODEL

A. Industrial Units as Building Blocks

Consider a complex industrial system, such as the one in Fig. 1(a). One can model this system as a combination of several industrial units of different sizes and types that work together to produce one or multiple final products. To model each unit, we need to first identify its inputs and outputs in terms of both material and energy, as shown in Fig. 1(b). We are particularly interested in the electricity energy inputs to industrial units, e.g., to run electric boilers, create electric arc, run electric motors, etc. Output energy, while not common for most units, is any *usable* energy form as a *by-product*.

The output material from one unit is often fed to another unit as input to go through a *multi-stage processing chain* before a final product is produced. As an example, in Fig. 1(a), we can identify two processing chains $1 \rightarrow 2 \rightarrow 3$ and $1 \rightarrow 4$ to produce final products m_6 and m_8, respectively. The raw materials are marked as m_1, m_2, and m_7. The units in a processing chain may or may not work simultaneously. However, it is always necessary to have enough input materials available at each unit, before it can start a new batch processing cycle.

Suppose time is divided into equal time slots, where each time slot is modeled by its *beginning* time. The numbers in parentheses inside each unit in Fig. 1(a) shows the number of time slots that the unit must operate to finish *one* batch cycle. Unit 3 is an *interruptible* load and its represented by a *circle*. If needed, its operation can be stopped in the middle of

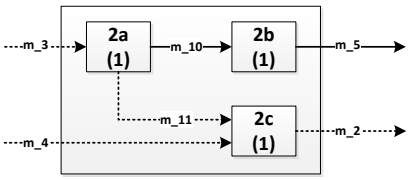

Fig. 2. Breaking down unit 2 in Fig. 1(a) into three physical subunits to reveal the option of operating subunit 3c separately from subunits 2a and 2b.

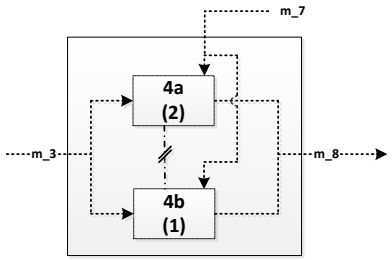

Fig. 3. Breaking down unit 4 in Fig. 1(a) into its two logical subunits in order to represent the ability of unit 4 to support variable batch cycles.

a batch cycle and restored later. In contrast, units 1, 2, and 4 are represented by *rectangles* because they are *uninterruptible*. The flow of material m_5 from unit 2 to unit 3 is shown with a *solid* line to highlight that due to its pressure, temperature, or other characteristics, material m_5 must be processed by unit 3 as soon as it is produced by unit 2. In contrast, a material flow with *dashed* line represents a material that does not have to be processed immediately; hence, it can be stored and used at a later time. Material m_2 is a usable *by-product* of unit 2 that is fed back to unit 1. Also note that materials m_1 and m_3 are consumed by multiple units. Finally, each unit may undergo *different number of cycles*. For example, unit 1 may undergo 3 cycles while units 2, 3, and 4 may undergo 2 cycles only.

B. Physical and Logical Subunits

An industrial unit can be a complex system, consisting of multiple internal *subunits* that conduct different *subtasks*. Understanding such internal details of a unit may sometimes reveal new potentials for load flexibility. For example, consider unit 2 in Fig. 1(a). This unit is uninterruptible and takes two time slots to finish one batch cycle. The input materials to this unit are m_3 and m_4. The output materials from this unit are m_5 and m_2. In practice, this unit may consist of three internal subunits 2a, 2b, and 2c, as shown in Fig. 2. Each subunit requires one time slot to finish operation. Based on the additional details that are now available about unit 2 in Fig. 2, it turns out that the uninterruptible feature of unit 2 is due to the way that subunits 2a and 2b operate, where there is a need to immediately process the internal material m_5 by subunit 2b. However, such requirement does *not* involve subunit 2c. Therefore, subunit 2c can operate *independently* from the other two subunits as long as its input materials are ready.

The definition of subunits for an industrial unit does not have to be based on the existence of physically separated equipment. In fact, one may also represent the internal operational details of a unit by introducing some *logical* subunits. For example, one may use logical subunits to model *variable batch cycles*. This option is illustrated in Fig. 3. Suppose we now know that unit 4 takes two time slots to finish operation but only if it works at full capacity. Further suppose it turns out that unit 4 can also operate in half capacity and in that case it would take only 1 time slot to finish operation. Accordingly, logical subunit 4a represents unit 4 when it operates at full capacity and logical subunit represents unit 4 when it operates at half capacity. Here, the *dashed-dot line with two crossing lines* between subunits 4a and 4b indicates exclusive operation because only one setting can be scheduled at a time.

Note that, as far as our overall methodology in this paper is concerned, *there is no difference between units and subunits*. That is, once all units and subunits are defined based on the intended granularity and their characteristics are understood and modeled, we can then simply refer to all of them as units. Accordingly, based on the conventions that we defined in Section II-A to characterize units, one can represent a subunit as a *circle* or *square*. The interactions between subunits can also be represented in form of *solid* or *dashed* lines.

We must also point out that once we break down a unit into its physical or logical subunits, we may no longer consider the original unit in our model. For example, once we replace unit 2 in Fig. 1(a) with subunits 2a, 2b, and 2c, then the set of units in the system becomes 1, 2a, 2b, 2c, 3, and 4. If we also replace unit 4 with subunits 4a and 4b, then the set of units in the system becomes 1, 2a, 2b, 2c, 3, 4a, and 4b.

III. Problem Formulation

One can *shape* the electric load profile of an industrial load by adjusting the *operational schedule* of its batch processing units subject to their operational needs and inter-operational sequences. In this section, we formulate the design objective, decision variables, and constraints in an optimal ILC problem.

A. Objective Function

The primary goal of any industry is to maximize its profit, i.e., its *revenue* minus *cost*. On one hand, revenue depends on the amount and sale price of each final product. On the other hand, cost depends on the amount and purchase price of raw materials and also the operational cost of industrial units, including their cost of electricity. Therefore, we have

$$\text{Profit} = \text{Revenue} - \text{Cost}, \tag{1}$$

where

$$\text{Revenue} = \sum_{f \in \mathcal{F}} m_f[T] p_f, \tag{2}$$

and

$$\begin{aligned} \text{Cost} = & \sum_{r \in \mathcal{R}} \left(m_r[0] - m_r[T] \right) p_r \\ & + \sum_{t=1}^{T} \sum_{k \in \mathcal{K}} m_k[t] \gamma_k + C_{fixed} + C_{elct}. \end{aligned} \tag{3}$$

The first term in (3) is the total cost of raw materials consumed during the scheduling horizon. The second term is the total

cost of storing materials of any type. The third term is any fixed cost that does not depend on our decision variables, e.g., cost of labor, facility, etc. Finally, and most importantly, the fourth term is the *cost of electricity*, which we explain next.

B. Cost of Electricity

The cost of electricity depends on both the electric load profile and the pricing method used by the utility company.

1) Day-Ahead Pricing (DAP): This pricing method is used, e.g., by Ameren Inc. in Illinois [23]. In DAP, the utility releases the hourly prices for the next day on a daily basis. Let $p[t]$ \$/kWh denote the day-ahead price of electricity at time slot t. Also let $L[t]$ denote the *total* power consumption at the industrial complex of interest at time slot t. We have:

$$C_{elct} = \sum_{t=1}^{T} L[t]p[t], \tag{4}$$

where T is the scheduling horizon.

2) Time-of-Use Pricing (ToUP): This pricing method is used, e.g., by Pacific Gas & Electric in California for commercial and industrial users [24]. In ToUP, there are multiple rate periods as *on-peak*, *mid-peak*, and *off-peak* hours. Prices are usually fixed over a season. Mathematically, ToUP is a special case of DAP; therefore, the cost of electricity when ToUP is used is formulated similar to the expression in (4).

3) Peak Pricing (PP): This pricing method is used, e.g., by Riverside Public Utilities in California [25]. It usually has two components: *usage charge* and *peak demand charge*. Usage charge is based on flat or time-of-use rates. It can be modeled as in (4). Peak demand charge is rather based on the consumer's daily or monthly peak load. It is calculated by measuring electricity usage at the hour of the day or month during which the consumer's load is at its highest amount. The peak price, denoted by p_{pd} \$/kWh, is usually much higher than the prices that are used to calculate the usage charge. That is, $p_{pd} \gg p[t]$ for all $t \in \mathcal{T}$. As a result, PP can encourage users to consume electricity more *uniformly* during the day in order to improve the *load factor*. The cost of electricity when PP method is used can be calculated as

$$C_{elct} = \sum_{t=1}^{T} L[t]p[t] + \left(\max_{t} L[t]\right) p_{pd}. \tag{5}$$

4) Inclining Block Rates (IBR): This pricing method is another way to encourage balanced load profiles. It also encourages energy conservation. It is offered, e.g., by British Columbia Hydro in Canada to industrial users [7]. In IBR pricing, beyond a certain load *threshold*, the price increases to a higher value. In a typical two-tier IBR model, we have [7]:

$$p[t] = \begin{cases} p_{bl}[t] & \text{if } L[t] \le L_0[t], \\ p_{hl}[t] & \text{if } L[t] > L_0[t], \end{cases} \tag{6}$$

where $p_{bl}[t]$, $p_{hl}[t]$, and $L_0[t]$ are the price parameters at time t. If $L[t] \le L_0[t]$, then the cost of electricity at time t becomes

$$C_{elct}[t] = p_{bl}[t]L[t]. \tag{7}$$

Otherwise, i.e., if $L[t] > L_0[t]$, we have

$$C_{elct}[t] = p_{bl}[t]L_0[t] + (L[t] - L_0[t])\, p_{hl}[t]. \tag{8}$$

The total cost of electricity during an interval of interest $[1, T]$ under IBR pricing is calculated as $C_{elct} = \sum_{t=1}^{T} C_{elct}[t]$.

5) Critical Peak Pricing (CPP): This pricing method is used, e.g., by Fort Collins Utilities in Fort Collins, CO [26]. In CPP, there is an additional charge during the hours where the utility experiences spikes in the total load demand in its service territory. Since CPP depends on the *combined behavior* of all consumers, individual customers are unaware of its happening time. Therefore, utilities send *warnings* from 5 minutes to 24 hours in advance to inform users about the occurrence of an upcoming critical peak hour. The exact setup of CPP may vary in different places. In this paper, we assume that the CPP price p_{cp} \$/kWh and the start and duration of each critical peak hour are announced as part of the warning signal sent by the utility. Following the analysis of historical CPP warnings in [27], we assume that warnings accurately identify the critical peak hour, i.e., no CPP false alarm may be sent to consumers.

Similar to PP, CPP is usually combined with usage charges. The cost of electricity under CPP pricing methods becomes

$$\sum_{t=1}^{t_{beg}-1} L[t]p[t] + \sum_{t=t_{beg}}^{t_{end}} L[t]p_{cp} + \sum_{t=t_{end}+1}^{T} L[t]p[t], \tag{9}$$

where t_{beg} and t_{end} denote the beginning and the end of the critical peak time frame, where $t_{beg} < t_{end}$. The CPP price is usually much higher than the regular usage price and even peak price. As reported in [27], when CPP is used, at least 23% of the cost of electricity comes from the CPP charges.

Note that, in this paper, we consider the typical scenario where the industrial facility procures electricity from a local utility company at a price that depends on the pricing method as we discussed earlier. However, given the large electricity usage of industrial loads, it is also feasible for industrial facilities to participate in the wholesale electricity market and procure their needed electricity by submitting proper demand bids. This option is available in practice, e.g., in California in the United States. For more details please refer to [28]–[30].

C. Decision Variables

The decision variables in our proposed problem formulation and the range of the values that they can take are as follows:

$$\begin{aligned}
&s_i[t] \in \{0, 1, 2, ...\}, && \forall i, \forall t, \\
&e_i[t] \in \{0, 1, 2, ...\}, && \forall i, \forall t, \\
&x_i[t] \in \{0, 1\}, && \forall i, \forall t, \\
&u_i[t] \in \{0\} \cup [\alpha_i, \beta_i], && \forall i, \forall t, \\
&y_i[t] \ge 0, && \forall i, \forall t, \\
&m_k[t] \in [0, \eta_k], && \forall k, \forall t, \\
&l_i[t] \ge 0, && \forall i, \forall t.
\end{aligned} \tag{10}$$

The definitions of the above variables are given in the nomenclature. Next, we explain these variables and their relationship.

D. Batch Cycle's Start and End Time Constraints

As listed in the nomenclature, $s_i[t]$ denotes the number of unit i's batch cycles that started before or at time slot t. Similarly, $e_i[t]$ denotes the number of unit i's batch cycles that ended before or at time slot t. These two sets of variables are defined in order to keep track of the start time and the end time of each batch cycle in each unit. By definition, we have:

$$0 \leq s_i[t] - s_i[t-1] \leq 1, \quad \forall i, \forall t, \tag{11}$$

$$0 \leq e_i[t] - e_i[t-1] \leq 1, \quad \forall i, \forall t, \tag{12}$$

where for each unit i the initial condition is defined as $s_i[0] = e_i[0] = 0$. If at a time slot t we have $s_i[t] - s_i[t-1] = 1$, then unit i has started a *new* cycle at time slot t and if $e_i[t] - e_i[t-1] = 1$, then unit i has finished a cycle at time slot t. Since a unit may not start a new cycle unless its current cycle has ended, the following inequalities must hold:

$$0 \leq s_i[t] - e_i[t] \leq 1, \quad \forall i, \forall t. \tag{13}$$

Note that, if $s_i[t] - e_i[t] = 0$, then $s_i[t] = e_i[t]$, i.e., all batch cycles that started before or at time slot t also finished before or at time slot t. If $s_i[t] - e_i[t] = 1$, then the current cycle is *in process* and it has not finished yet. The following terminal conditions also need to hold in order to assure that all batch cycles for all units end before the end of the decision horizon:

$$s_i[T] = e_i[T], \quad \forall i. \tag{14}$$

Last but not least, we need to enforce the following terminal constraint on $x_i[t]$ for each unit i to complement the constraints in (14) such that no unit operates at the last time slot $t = T$ and that time is used only for delivering final products:

$$x_i[T] = 0, \quad \forall i. \tag{15}$$

E. Batch Cycle's Operational Constraints

Next, we need to relate variables $s_i[t]$ and $e_i[t]$ to $x_i[t]$ which is the primary variable to control the operation of each unit i. Let parameter a_i denotes the number of time slots that unit i must operate to finish one batch cycle. Then

$$s_i[t] = \begin{cases} 0, & \text{if } \sum_{j=1}^{t} x_i[j] = 0 \\ 1, & \text{if } 1 \leq \sum_{j=1}^{t} x_i[j] \leq a_i \\ 2, & \text{if } a_i + 1 \leq \sum_{j=1}^{t} x_i[j] \leq 2a_i \\ \vdots & \end{cases} \quad \forall i, \forall t \tag{16}$$

and

$$e_i[t] = \begin{cases} 0, & \text{if } 0 \leq \sum_{j=1}^{t} x_i[j] \leq a_i - 1 \\ 1, & \text{if } a_i \leq \sum_{j=1}^{t} x_i[j] \leq 2a_i - 1 \\ 2, & \text{if } 2a_i \leq \sum_{j=1}^{t} x_i[j] \leq 3a_i - 1 \\ \vdots & \end{cases} \quad \forall i, \forall t \tag{17}$$

After reordering the terms, we can replace (16) and (17) with the following equivalent but more tractable constraints:

$$(s_i[t] - 1)a_i + 1 \leq \sum_{j=1}^{t} x_i[j] \leq s_i[t]a_i, \quad \forall i, \forall t, \tag{18}$$

$$e_i[t]a_i \leq \sum_{j=1}^{t} x_i[j] \leq (e_i[t] + 1)a_i - 1, \quad \forall i, \forall t. \tag{19}$$

F. Exclusive Operation and Variable-Length Batch Cycles

Recall from Section II-B that some units might be required to operate exclusively. That is, for various reasons, certain units may not operate at the same time. Such operational requirement can be enforced by using the following constraints:

$$\sum_{i \in \mathcal{X}} x_i[t] \leq 1, \quad \forall \mathcal{X}, \forall t, \tag{20}$$

where $\mathcal{X} \subset \mathcal{V}$ is any set of units that must operate exclusively. For example, for the logical subunits in Fig. 3, we can define $\mathcal{X} = \{4a, 4b\}$. Accordingly, the constraint in (20) becomes

$$x_{4a}[t] + x_{4b}[t] \leq 1, \quad \forall t. \tag{21}$$

Thus, as intended, subunits 4a and 4b cannot operate simultaneously. To facilitate variable-length batch cycles, we also set:

$$\beta_{4a} = \beta_4, \ \beta_{4b} = \frac{1}{2}\beta_4, \ a_{4a} = a_4, \ a_{4b} = \frac{1}{2}a_4. \tag{22}$$

All other parameters for subunits 4a and 4b are then *inherited* from unit 4. If subunit 4a is scheduled, then it is as if unit 4 is scheduled to operate at full capacity, where its operation will take two time slots to finish. And if subunit 4b is scheduled, then it is as if unit 4 is scheduled to operate at half capacity, where its operation will take only one time slot to finish.

G. Input and Output Timing Constraints

For a unit that operates in batch cycles, it may import its input materials only at the *beginning* of its batch cycles. Recall from Section III-D that time slot t is the beginning of a batch cycle for unit i if and only if $s_i[t] - s_i[t-1] = 1$. Therefore, to assure the right timing of material entrance to unit i, the amount of materials entering unit i at time slot t denoted by $u_i[t]$ must satisfy $u_i[t] \in [\alpha_i, \beta_i]$ if $s_i[t] - s_i[t-1] = 1$, and $u_i[t] = 0$ if $s_i[t] - s_i[t-1] = 0$. This can be equivalently expressed in form of the following linear inequality constraints:

$$u_i[t] \geq (s_i[t] - s_i[t-1])\,\alpha_i, \quad \forall i, \forall t, \tag{23}$$

$$u_i[t] \leq (s_i[t] - s_i[t-1])\,\beta_i, \quad \forall i, \forall t. \tag{24}$$

Similarly, each unit may export its output materials only at the *end* of its batch cycles. Recall from Section III-D that time slot t is the end of a batch cycle for unit i if and only if $e_i[t] - e_i[t-1] = 1$. Also recall that all events happen at the beginning of a time slot and hence, it is assumed that output materials are produced at the beginning of the next time slot when a cycle ends. Therefore, to assure the right timing of material exit from unit i, the amount of materials exiting from unit i at time slot t denoted by $y_i[t]$ must satisfy $y_i[t+1] \geq 0$ if $e_i[t] - e_i[t-1] = 1$, and $y_i[t+1] = 0$ if $e_i[t] - e_i[t-1] = 0$ for all $t \in [1, T)$. This can be equivalently expressed in form of the following linear inequality constraints:

$$y_i[t+1] \geq 0, \quad \forall i, \forall t < T, \tag{25}$$

$$y_i[t+1] \leq \Omega\,(e_i[t] - e_i[t-1]), \quad \forall i, \forall t < T, \tag{26}$$

where $\Omega \gg 0$ is a large enough number. Finally, the following constraints assure that no material may leave any unit at the very beginning of the decision process, i.e., at time $t = 1$:

$$y_i[1] = 0, \quad \forall i. \tag{27}$$

H. Material Balance and Proportionality Constraints

The requirement for material balance in each unit is defined as the equality between the total amount of input materials that enter the unit at the beginning of each batch cycle and the total amount of output materials, including any waste, that leave the unit at the end of the same batch cycle. Since materials enter a unit only at the beginning of batch cycles and leave the unit only at the end of batch cycles, the above definition can be mathematically expressed in form of the following constraints:

$$\sum_{j=1}^{t} y_i[j+1]\left(e_i[j]-e_i[j-1]\right) = \sum_{j=1}^{t} u_i[j]\left(e_i[j]-e_i[j-1]\right), \quad \forall i, \forall t.$$

The above constraints require that by the end of each batch cycle, the total material that enters the unit must match the total material that leaves the unit. These nonlinear constraints can be replaced by the following equivalent linear constraints:

$$\begin{aligned} 0 &\le \sum_{j=1}^{t} u_i[j] - \sum_{j=1}^{t} y_i[j+1] \\ &\le \Omega\left(1-e_i[t]+e_i[t-1]\right), \quad \forall i, \forall t < T, \end{aligned} \tag{28}$$

Besides material balance in each unit, material balance should hold also across all units. That is, we need to have:

$$m_k[t] = m_k[t-1] + \sum_{i\in\mathcal{I}_k^{out}} q_i^k y_i[t] - \sum_{i\in\mathcal{I}_k^{in}} r_i^k u_i[t], \quad \forall k, \forall t, \tag{29}$$

where $m_k[0]$ is the amount of material k that is initially available in the storage. Note that, for each industrial unit i, we have $\sum_{k\in\mathcal{K}} r_i^k = 1$ and $\sum_{k\in\mathcal{K}} q_i^k = 1$. Constraint (29) is valid for all types of materials including non-storable materials.

I. Material Storage Constraints

The amount of each material k stored at any time may not exceed the capacity of its corresponding storage tank η_k. Also the amount of each material k stored at any time cannot be negative. These constraints can be formulated as

$$0 \le m_k[t] \le \eta_k, \quad \forall k, \forall t. \tag{30}$$

Next, recall from Section II that certain materials cannot be stored. Rather they must be immediately sent to the next unit along the processing chain. Let $\mathcal{K}_{imd}$ denote the set of materials with such requirements. We need to have:

$$\eta_k = 0, \quad \forall k \in \mathcal{K}_{imd}. \tag{31}$$

From (31) and (30), we have $m_k[t] = 0$, $\forall k \in \mathcal{K}_{imd}$ and $\forall t$.

We also need specific constraints with respect to the storage of final products. Without loss of generality, we assume that storage facilities of final products are initially empty and final products of each cycle are accumulated until the end of scheduling horizon. Therefore, $m_f[T]$ indicates the sum of final products f that are produced during the load scheduling horizon. The following captures the production requirement:

$$m_f[T] \ge \phi_f, \quad \forall f \in \mathcal{F}. \tag{32}$$

J. Constraints for Uninterruptible Units

While there exist industrial units, e.g., in the automotive industry, whose operations can be interrupted and later restored, there are also units, e.g., in chemical industries, whose operations *cannot* be interrupted. Once an uninterruptible unit starts a batch cycle, it may not stop operation until it finishes its current batch cycle. Mathematically, this means that if $s_i[t] - s_i[t-1] = 1$, then we must have $x_i[t] = x_i[t+1] = \cdots = x_i[t+a_i-1] = 1$. To model this mathematically, first, we note that a batch cycle for an uninterruptable load may start anywhere between time slots $t = 1$ and $t = T - a_i + 1$; otherwise, the batch cycle does not finish by the end of the load scheduling horizon at time $t = T$. Therefore, in order to assure the proper operation of an uninterruptable unit, the following constraints must hold for any $j = 0, 1, \ldots, a_i - 1$:

$$s_i[t] - s_i[t-1] \le x_i[t+j], \forall i \in \mathcal{I}_{unt}, \forall t \in [1, T-j]. \tag{33}$$

Note that, if at a time slot t, we have $s_i[t] - s_i[t-1] = 1$, then (33) becomes $1 \le x_i[t+j]$, for all $j = 0, 1, \ldots, a_{i-1}$. That is, $x_i[t] = x_i[t+1] = \ldots = x_i[t+a_i-1] = 1$.

K. Electricity Consumption Constraints

In general, the amount of power consumption at an industrial unit depends on whether the unit is *operating* or it is on *stand-by* and also the amount of material that is loaded into the unit during its operation. In this regard, we can model

$$l_i[t] = \begin{cases} l_i^{min} & \text{if } x_i[t] = 0 \\ c_i M_i[t] + d_i & \text{if } x_i[t] = 1 \end{cases} \quad \forall i, \forall t, \tag{34}$$

where the notations are defined in the nomenclature and

$$M_i[t] = \sum_{j=1}^{t} u_i[j] - \sum_{j=1}^{t} y_i[j] \tag{35}$$

denotes the total amount of all materials that is inside unit i at time slot t. We can replace (34) with the following constraints:

$$l_i[t] \ge l_i^{min}, \quad \forall i, \forall t, \tag{36}$$

$$l_i[t] \ge c_i M_i[t] + d_i - \Omega\left(1 - x_i[t]\right), \quad \forall i, \forall t, \tag{37}$$

where Ω is a large enough number. Assuming that for each unit i, we have $l_i^{min} \le d_i$, we can explain (36) and (37) as follows. If $x_i[t] = 1$, then (36) and (37) reduce to $l_i[t] \ge c_i M_i[t] + d_i$. And if $x_i[t] = 0$, then (36) and (37) reduce to $l_i[t] \ge l_i^{min}$.

Based on the above explanations, the total power consumption across all units in the industrial complex becomes:

$$L[t] = \sum_{i\in\mathcal{V}} l_i[t] + l_{back}[t], \tag{38}$$

where $l_{back}[t]$ is known and denotes the background load which includes the facility loads (such as lighting and HVAC) and non-controllable loads (such as units that operate continuously). Recall that this amount has to be upper bounded:

$$L[t] \le L_{max}, \quad \forall t, \tag{39}$$

where L_{max} is determined based on the type of the meter and electric feeder that the industrial complex is connected to.

L. Profit Maximization Problem

We are now ready to formulate the following profit maximization problem for the purpose of energy consumption scheduling for industrial complexes and industrial processes:

$$\begin{aligned} \underset{(10)}{\textbf{Maximize}} \quad & \sum_{f\in\mathcal{F}} m_f[T]\, p_f - \sum_{r\in\mathcal{R}} \left(m_r[0] - m_r[T]\right)\, p_r \\ & - \sum_{t=1}^{T} \sum_{k\in\mathcal{K}} m_k[t]\, \gamma_k - C_{fixed} - C_{elct} \end{aligned} \tag{40}$$

$$\textbf{Subject to} \quad (11)-(15), (18)-(33), (36)-(37), (39).$$

Note that, depending on the exact pricing model being applied, we replace C_{elct} in (40) with one of the electricity cost models in (4) to (9). However, regardless of the choice of the electricity cost model, the optimization problem in (40) is either a *mixed integer linear program* (MILP) or it can be easily converted to an MILP; therefore, it can be solved efficiently and in a timely fashion using MILP optimization software, such as MOSEK [31] and CPLEX [32].

M. Behind-the-Meter Batteries and Renewable Generators

The problem formulation in (40) can easily be modified to also include batteries and renewable generators. To include batteries in the ILC problem, we introduce three new variables: $l_{ch}[t]$ and $l_{dch}[t]$ to indicate the charge and discharge rates of the battery system at slot time t, respectively, and $b[t] \in \{0, 1\}$ to indicate if the battery is charged or discharged at time slot t. If $b[t] = 1$, then the battery is charged at time slot t, and if $b[t] = 0$, then the battery is discharged. It is required that

$$0 \le l_{ch}[t] \le b[t] l_{ch}^{max}, \quad \forall t, \tag{41}$$

$$0 \le l_{dch}[t] \le (1 - b[t]) l_{dch}^{max}, \quad \forall t, \tag{42}$$

where l_{ch}^{max} and l_{dch}^{max} denote the maximum charge rate and the maximum discharge rate of the batteries, respectively. Since the batteries cannot be discharged if they are empty and they cannot be charged if they are full, the following constraints are also needed in the problem formulation:

$$0 \le B^{init} + \sum_{j=1}^{t} \left(\mu\, l_{ch}[j] - \theta\, l_{dch}[j]\right) \le B^{full}, \quad \forall t, \tag{43}$$

where B^{init} and B^{full} denote the initial charge level and the full charge capacity of the battery system, respectively. Here, $\mu \le 1$ and $\theta \ge 1$ denote the efficiency of the battery system during charge and discharge, respectively.

Besides adding constraints (41)-(43) to the the problem in (40), we also need to slightly revise the load models in (38) in order to incorporate the impact of adding on-site batteries:

$$L[t] = \sum_{i\in\mathcal{V}} l_i[t] + l_{back}[t] + l_{ch}[t] - l_{dch}[t], \quad \forall t. \tag{44}$$

In general, $L[t]$ in (44) may take both positive and negative values. In particular, $L[t]$ can be negative if the rate at which the battery is discharged at time t is higher than the total power consumption at the industrial complex at time t. If $L[t] < 0$, then it means that the industrial complex is injecting power back to the grid. Depending on the policies set forth by the regional utility company that feeds the industrial complex, a back injection power may or may not be allowed, as some protection devices on distribution systems may not support back injections. In that case, it is required to also add the following constraints into the problem formulation:

$$L[t] \ge 0, \quad \forall t. \tag{45}$$

Finally, suppose the industrial complex is equipped with local renewable generator and renewable generator outputs are predicted accurately at each time slot. In that case, equation (44) should be slightly revised as follows:

$$L[t] = \sum_{i\in\mathcal{V}} l_i[t] + l_{back}[t] + l_{ch}[t] - l_{dch}[t] - l_{slr}[t], \quad \forall t, \tag{46}$$

where $l_{slr}[t]$ is the expected available solar energy at time t.

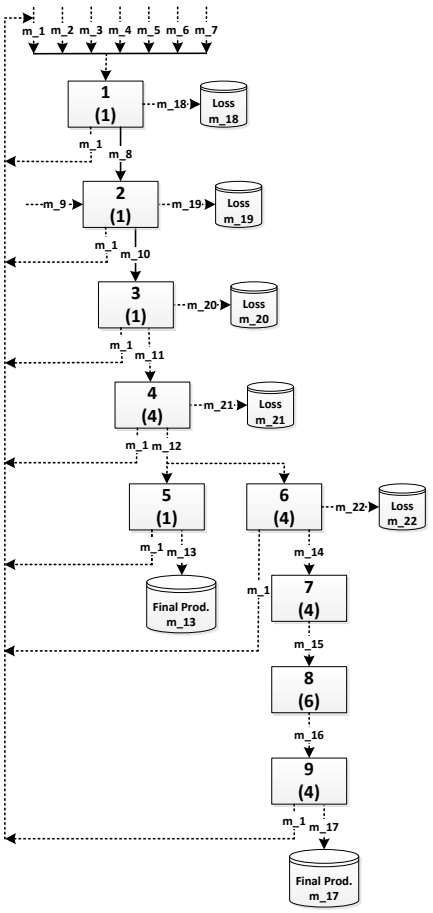

Fig. 4. The flow diagram and interacting units for a steel mill industry.

IV. Case Studies

Steel mill industry is energy intensive, and electricity cost accounts for a big portion of the total operational cost [33]. Fig. 4 shows flow diagram of a steel mill [34], [35]. The names of units and materials in a typical still mill are given in Table II. For each unit in Fig. 4, the number inside parenthesis indicates the duration of each batch cycle. These numbers were chosen through consulting with the California Steel Industry in Fontana, CA in the United States and the Esfahan Steel Company in Isfahan, Iran, with some modifications.

TABLE II
NAME OF UNITS AND MATERIALS IN FIG. 4.

Units	Materials	
1: Arc Furnace	m_1: Home Scrap	m_{10}: Treated Steel
2: Ladle Furnace	m_2: Purchased Scrap	m_{11}: Cast Steel
3: Slab Caster	m_3: DRI	m_{12}: Hot Band
4: Hot Strip Mill	m_4: Lime	m_{13}: Hot Band (F)
5: Skin Pass Mill	m_5: Alloys	m_{14}: Pickled Band
6: Pickle Line	m_6: Refractory	m_{15}: Cold Rolled
7: Cold Mill	m_7: Electrode	m_{16}: Annealed Band
8: Annealing Line	m_8: Liquid Steel	m_{17}: Cold Rolled (F)
9: Finishing Mill	m_9: Carbon	$m_{18} - m_{22}$: Losses

TABLE III
PARAMETERS IN INDUSTRIAL UNITS IN THE CASE STUDY.

i	α_i	β_i	c_i	d_i
1	10	100	3.911	0.001
2	8	80	0.135	0.001
3	30	300	0.198	0.001
4	100	1000	1.023	0.001
5	4	40	0.047	0.001
6	40	400	0.228	0.001
7	40	400	0.340	0.001
8	60	600	0.140	0.001
9	40	400	0.181	0.001

The parameters related to the operation and energy consumption of each unit are shown in Table III. Here, α_i and β_i are in metric tonne, c_i is in GJ/tonne, and d_i is in GJ.

Proportionality of input materials of unit 1 are 0.125, 0.376, 0.442, 0.036, 0.005, 0.014, and 0.002, and proportionality of input materials of unit 2 are 0.9996 and 0.0004, respectively [34]. Proportionality of output materials of unit 1 are 0.02, 0.79, 0.19. Proportionality of output materials of unit 2 are 0.021, 0.965, and 0.014. Proportionality of output materials of unit 3 are 0.049, 0.941, and 0.01. Proportionality of output materials of unit 4 are 0.025, 0.965, and 0.01. Proportionality of output materials of unit 5 are 0.01 and 0.99. Proportionality of output materials of unit 6 are 0.03, 0.95, and 0.02. Proportionality of output materials of unit 9 are 0.050 and 0.950.

Storage capacity for all materials is chosen to be 20,000 tonnes, except for material 8 and 10 which must be zero because these materials may not be stored. The initial amount is set to zero for all non-raw materials, 10,000 tonnes for material 1, and 20,000 tonnes for every other raw material. There is no cost to store materials. The unit prices of the initial materials are 0, 127.84, 163.54, 3.96, 5.85, 9.1, 11.6, and 10 \$/tonne, respectively. The unit prices of the final products are 710, 750, and 0 \$/tonne, respectively [36]–[38]. The daily background load in gigajoules is chosen to be 0.06 for hours 1 and 21 to 24, 0.05 for hours 2 to 6, 0.09 for hours 7 and 10 to 12, 0.1 for hours 8 and 9, 0.08 for hours 13 to 18, and 0.07 for hours 19 and 20. Capacity, initial charge level, maximum charge rate, and maximum discharge rate of the battery system are 5000 kWh, 1500 kWh, 2500 kWh/hour, and 2500 kWh/hour (i.e., c-rate of 0.5), respectively. The load control horizon is $T = 48$ time slots (hours) and L_{max} is chosen to be 5×10^5 kWh. The minimum needed final products are chosen to be 20, 40, and 0 tonnes, respectively.

The electricity price data for DAP is from PJM, starting March 20, 2014 [39]. To make different pricing methods comparable, we used DAP as reference and set the parameters for other pricing methods accordingly. Solar data is from [40], which includes one sunny day followed by a cloudy day. For the *no load control* case, problem (40) is solved for some flat electricity prices, which are calculated as follows: in DAP and CPP, the average of DAP price; in ToUP, the average of off-peak and on-peak prices; in IBR, the average of base-load and high-load prices; and in PP, the average of regular price.

In all cases, the profit maximization problem in (40) was solved using CPLEX [32]. The relative mixed-integer programming gap tolerance is set to 3% in this case.

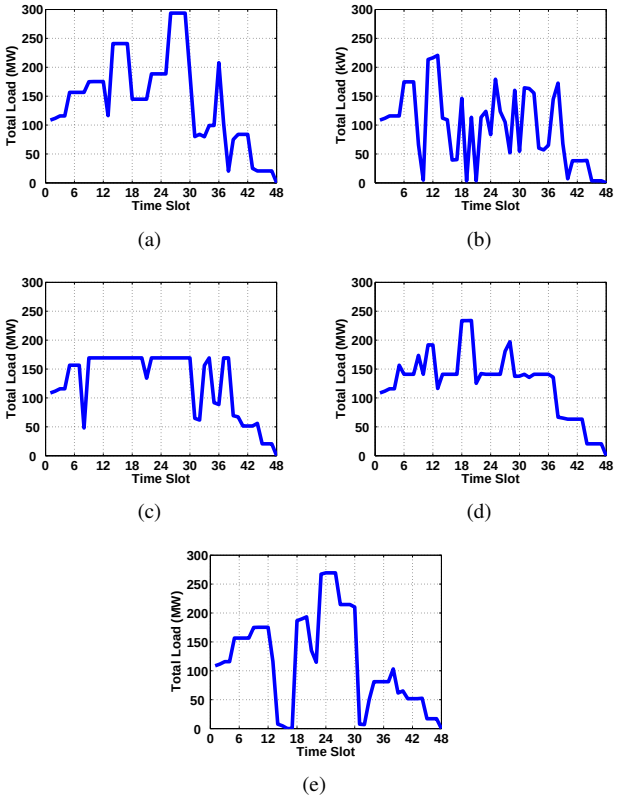

Fig. 5. Optimal load profile: (a) DAP; (b) ToUP; (c) PP; (d) IBR; (e) CPP.

A. Impact of Pricing on Load Profile

The load profiles for different pricing models are shown in Fig. 5. We can see that the choice of pricing mechanism can significantly affect the optimal demand response of the steel industry. Note that, the areas under the curves in Fig. 5 are *not* the same. For example, the total energy usage under DAP in Fig. 5(a) is 6.76 GWh while the total energy usage under CPP in Fig. 5(e) is 5.54 GWh. This is because, besides optimizing power usage, here, we also optimize material usage as well as the amount of final product(s). As a result, the changes in the price of electricity can affect the amount of material flow and final product(s); accordingly, different optimal energy usage levels could be resulted under different pricing scenarios.

It is interesting to also calculate the average fraction of material that was loaded to each unit during its operation, over the capacity of the unit. The results are Fig. 6 for all

nine units. The results in this figure are for the DAP case. Similar numbers can be obtained for other pricing methods.

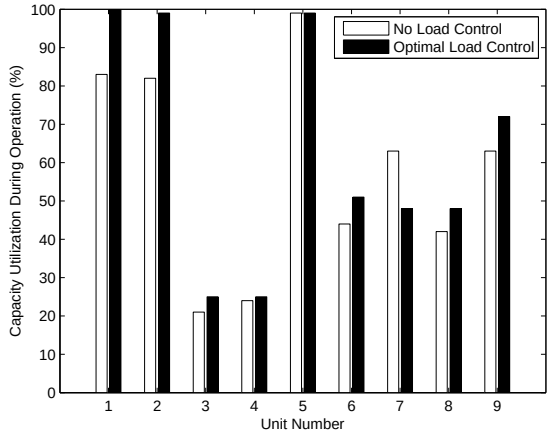

Fig. 6. The material capacity utilization for each unit with and without load control under DAP. The number of units are based on Table II.

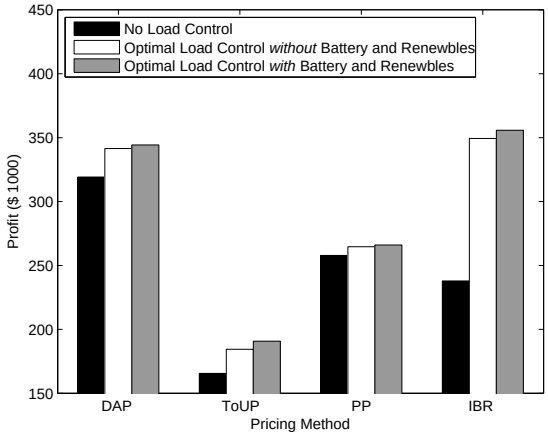

Fig. 7. Profit under different price and resource scenarios.

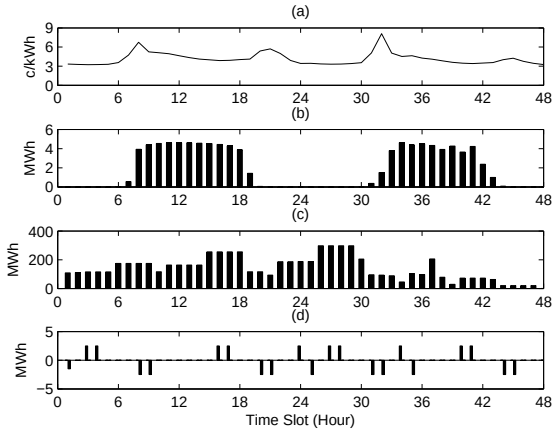

Fig. 8. Operation with battery and renewable generator: (a) the retail price of electricity, (b) solar generation, (c) controllable load, (d) battery schedule.

B. Advantages of Optimal Load Control

From Fig. 7, in each pricing model, optimal scheduling results in higher profit. The improvement is 45% under IBR and 10% under ToUP. The use of behind-the-meter battery and renewable generator can further increase profit. However, since the total electricity usage of the units is much larger than the available renewable energy and the battery size, the profit improvement is small compared to the case with no battery and renewable energy. From Fig. 8, the battery is charged at low-price time slots and discharged at high-price time slots.

Figs. 9(a) and (b) show the impact of battery capacity and battery efficiency on profit, respectively. We can see that profit increases as the battery capacity or battery efficiency increase.

The above results demonstrate some of the advantages of our proposed ILC compared to the existing ILC methods in the literature. First, unlike in [16], [19]–[22], here, *batch-size* of each unit is a decision variable and the objective function is *profit* which is more appropriate for industrial consumers. Second, unlike in [16], [20] where the industrial units are scheduled to operate for exactly one cycle during the scheduling horizon, here, each unit may undergo *multiple cycles* during the scheduling horizon, where the number of cycles for each unit is in fact an optimization variable. Finally, the existing literature does not incorporate interruptibility of industrial units, material scheduling, or material feedback.

C. Variable Batch Cycles

Recall from Sections II-B and III-F that some units may allow variable-length batch cycles. This may create additional load flexibility to increase profit. To see this, suppose units 4 and 6 allow variable-length batch cycle. Unit 4 can now operate at either full capacity that takes four time slots to finish or half capacity that takes two time slots. Similarly, unit 6 can now operate at either full capacity that takes four time slots to finish or half capacity that takes two time slots. In that case, the optimal operation of the steel mill under DAP would result in the total load profile that is shown in Fig. 10. This figure is comparable with Fig. 5(a), where the operation of all units had fixed length. We can see that the load profiles are different in the two figures. The total energy usage under fixed and variable batch cycles is 6.67 GWh and 5.85 GWh, respectively. As for the total profit, it has increased from $314K under fixed batch cycles to $388K under variable batch cycles.

The operation of units 4 and 6 under fixed batch cycles and variable batch cycles are compared in Fig. 11. We can see that the operation of both units have changed under batch variable-length batch cycles. The changes for unit 4 are particularly significant, where the first few and last few batch cycles operate are at half capacity. As for the case of unit 6, one full capacity cycle is moved to an earlier time and a new half capacity is added after that with one time slot gap in between. Note that, for unit 4, when it operates with variable cycles, we obtain $x_4[t] = x_{4a}[t] + x_{4b}[t]$, where logical subunits 4a and 4b operate exclusively. Similarly, for unit 6 when it operates with variable cycles, we obtain $x_6[t] = x_{6a}[t] + x_{6b}[t]$, where logical subunits 6a and 6b operate exclusively.

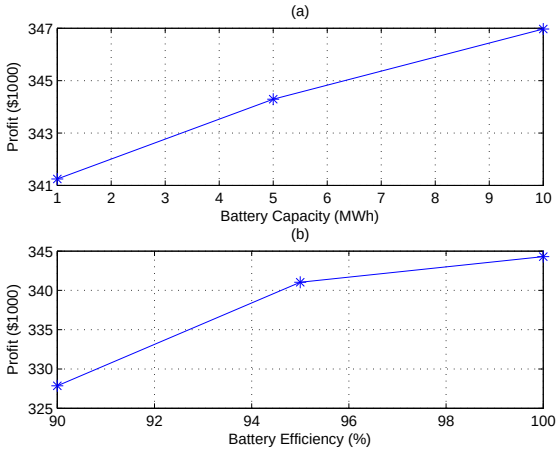

Fig. 9. The impact of battery parameters on profit: (a) capacity, (b) efficiency.

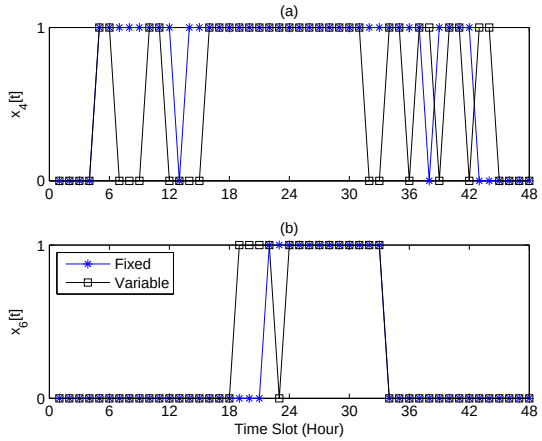

Fig. 11. Comparing fixed and variable batch cycles: (a) unit 4, (b) unit 6.

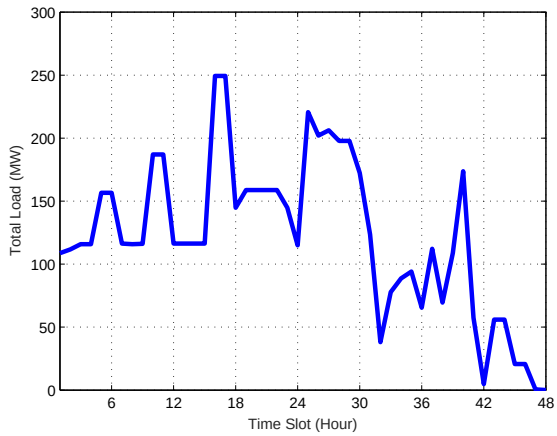

Fig. 10. Optimal load profile under variable cycles and DAP pricing.

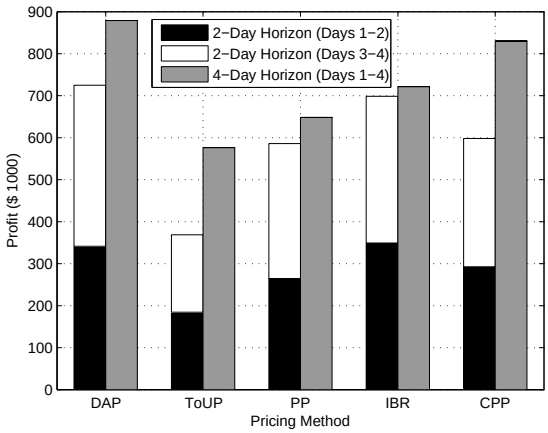

Fig. 12. Impact of longer scheduling horizons on the overall profit.

D. Longer Scheduling Horizons

From Fig. 12, the total profit increases as the scheduling horizon increases due to more time flexibility. The improvement under ToUP is over 50%, under CPP is around 40%, under DAP is over 20%, and under PP is over 10%.

E. Timing of CPP Warning

From Fig. 13, a late CPP warning can be very costly for an industrial load since an industrial load often does not have enough flexibility to change the operation of units in short notice, e.g., due uninterruptible nature of many units.

V. Conclusions

A new optimization-based industrial load control framework is proposed under five different smart pricing methods: DAP, ToUP, PP, IBR, and CPP. The formulated optimization problem is a tractable mixed-integer linear program. Various load features that are specific to industrial sector are considered, including inter-dependence among industrial units, operation across multiple days, size and number of batch processes, sequential operation, interruptible and uninterruptible operation, and joint energy management and material flow management. The use of behind-the-meter energy resources, such as on-site batteries and renewable generators, is also considered.

Case studies are presented in form of an illustrative example and also for a steel mill industry. It is shown that the choice of pricing mechanism can significantly affect the optimal demand response of an industrial load. The advantages of using local energy resources and the optimal sizes of these resources also depend on the choice of the pricing method that is being used. Due to the inter-dependency among industrial units, industrial load control can benefit from increasing the scheduling horizon to multiple days. However, such increase can come at the cost of higher computational complexity. Finally, it is beneficial to co-optimize energy usage and material flow, because controlling the material flow to each sub processing unit affects both revenue, by having impact on the amount of final products, and cost, by having impact on the amount of power consumption.

Acknowledgement

The authors would like to thank Ralph Hayden, the Chief Metallurgist at the California Steel Industry in Fontana, CA.

References

[1] C. Joe-Wong, S. Sen, S. Ha, and M. Chiang, "Optimized day-ahead pricing for smart grids with device-specific scheduling flexibility," *IEEE*

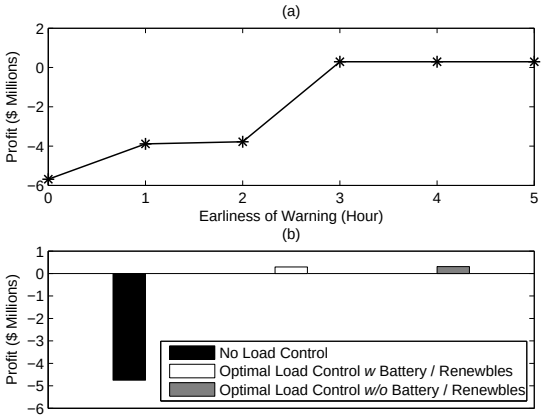

Fig. 13. Results under CPP pricing method: (a) profit versus the earliness of warning; (b) profit under different control and resource scenarios.

Journal on Selected Areas in Communications, vol. 30, no. 6, pp. 1075–1085, 2012.

[2] J. Sheen, C. Chen, and T. Wang, "Response of large industrial customers to electricity pricing by voluntary time-of-use in taiwan," in *IET Generation, Transmission and Distribution*, vol. 142, 1995, pp. 157–166.

[3] P. H. Jayantilal and N. Shah, "A review on electrical energy management techniques for supply and consumer side in industries," *Int. Journal of Scientific Engineering and Technology Research*, vol. 3, pp. 550–556, Apr. 2014.

[4] A. V. Stokke, G. L. Doorman, and T. Ericson, "An analysis of a demand charge electricity grid tariff in the residential sector," *Energy Efficiency*, vol. 3, no. 3, pp. 267–282, 2010.

[5] P. Samadi, H. Mohsenian-Rad, V. Wong, and R. Schober, "Tackling the load uncertainty challenges for energy consumption scheduling in smart grid," *IEEE Trans. on Smart Grid*, vol. 4, no. 2, pp. 1007–1016, 2013.

[6] A. Bego, L. Li, and Z. Sun, "Identification of reservation capacity in critical peak pricing electricity demand response program for sustainable manufacturing systems," *International Journal of Energy Research*, vol. 38, no. 6, pp. 728–736, 2014.

[7] A.-H. Mohsenian-Rad and A. Leon-Garcia, "Optimal residential load control with price prediction in real-time electricity pricing environments," *IEEE Trans. on Smart Grid*, vol. 1, no. 2, pp. 120–133, 2010.

[8] Y. Guo, M. Pan, and Y. Fang, "Optimal power management of residential customers in the smart grid," *IEEE Trans. on Parallel and Distributed Systems*, vol. 23, no. 9, pp. 1593–1606, 2012.

[9] T. Hubert and S. Grijalva, "Realizing smart grid benefits requires energy optimization algorithms at residential level," in *IEEE PES Conference on Innovative Smart Grid Technologies*, Anaheim, CA, Jan. 2011.

[10] A. H. Mohsenian-Rad, V. W. Wong, J. Jatskevich, R. Schober, and A. Leon-Garcia, "Autonomous demand-side management based on game-theoretic energy consumption scheduling for the future smart grid," *IEEE Trans. on Smart Grid*, vol. 1, no. 3, pp. 320–331, 2010.

[11] A. Raziei, K. P. Hallinan, and R. J. Brecha, "Cost optimization with solar and conventional energy production, energy storage, and real time pricing," in *IEEE PES Conference on Innovative Smart Grid Technologies*, Washington, DC, Feb. 2014.

[12] Z. Baharlouei, M. Hashemi, H. Narimani, and H. Mohsenian-Rad, "Achieving optimality and fairness in autonomous demand response: Benchmarks and billing mechanisms," *IEEE Trans. on Smart Grid*, vol. 4, no. 2, pp. 968–975, 2013.

[13] S. Kiliccote, M. Piette, and D. Hansen, "Advanced controls and communications for demand response and energy efficiency in commercial buildings," *Proc. of 2nd Carnegie Mellon CEPS*, Jan. 2006.

[14] S. A. Raziei and H. Mohsenian-Rad, "Optimal demand response capacity of automatic lighting control," in *IEEE PES Conference on Innovative Smart Grid Technologies*, Washington, DC, Feb. 2013.

[15] M. Ghamkhari and H. Mohsenian-Rad, "Energy and performance management of green data centers: A profit maximization approach," *IEEE Trans. on Smart Grid*, vol. 4, no. 2, pp. 1017–1025, 2013.

[16] A. Gholian, H. Mohsenian-Rad, Y. Hua, and J. Qin, "Optimal industrial load control in smart grid: A case study for oil refineries," in *Proc. of IEEE PES General Meeting*, Vancouver, Canada, Jul. 2013.

[17] C. A. Floudas and X. Lin, "Continuous-time versus discrete-time approaches for scheduling of chemical processes: a review," *Computers & Chemical Engineering*, vol. 28, no. 11, pp. 2109–2129, 2004.

[18] Y. Ding and S. H. Hong, "A model of demand response energy management system in industrial facilities," in *Proc. of IEEE SmartGridComm*, Vancouver, Canada, Nov. 2013.

[19] S. Bahrami, F. Khazaeli, and M. Parniani, "Industrial load scheduling in smart power grids," in *Proc. of IEEE CIRED*, 2013.

[20] S. Ashok and R. Banerjee, "An optimization mode for industrial load management," *IEEE Trans. on Power Systems*, vol. 16, no. 4, 2001.

[21] S. Ashok, "Peak-load management in steel plants," *Applied Energy*, vol. 83, no. 5, 2006.

[22] C. Babu and S. Ashok, "Peak load management in electrolytic process industries," *IEEE Trans. on Power Systems*, vol. 23, no. 2, 2008.

[23] https://www2.ameren.com/RetailEnergy/RtpDownload.

[24] http://www.pge.com/en/mybusiness/rates/tvp/toupricing.page.

[25] http://www.riversideca.gov/utilities/pdf/2013/Electric

[26] http://www.fcgov.com/utilities/business/rates/electric/coincident-peak.

[27] Z. Liu, A. Wierman, Y. Chen, B. Razon, and N. Chen, "Data center demand response: Avoiding the coincident peak via workload shifting and local generation," *ACM SIGMETRICS*, 2013.

[28] H. Mohsenian-Rad, "Optimal demand bidding for time-shiftable loads," *IEEE Trans. on Power Systems*, vol. 30, no. 2, pp. 939–951, 2015.

[29] M. Kohansal and H. Mohsenian-Rad, "Price-maker economic bidding in two-settlement pool-based markets: The case of time-shiftable loads," *IEEE Trans. on Power Systems (accepted)*, pp. 1–11, Mar. 2015.

[30] ——, "Extended-time demand bids: A new bidding framework to accommodate time-shiftable loads," in *Proc. of IEEE PES General Meeting*, Denver, CO, Jul. 2015.

[31] http://www.mosek.com.

[32] http://www-01.ibm.com/software/commerce/optimization/cplex-optimizer.

[33] http://www.worldsteel.org/dms/internetDocumentList/fact-sheets/fact_energy_2014/document/fact_energy_2014.pdf.

[34] http://calculatelca.com/wp-content/themes/athena/images/LCA

[35] United Nations Environment Programme, *Industry as a Partner for Sustainable Development: Iron and Steel*. UNEP/Earthprint, 2002, vol. 21.

[36] http://www.steelonthenet.com/cost-eaf.html.

[37] http://www.phoenixsteelservice.com.

[38] http://www.steelonthenet.com/steel-prices.html.

[39] http://www.pjm.com/markets-and-operations/energy/real-time/monthlylmp.aspx.

[40] http://www-metdat.llnl.gov/cgi-pub/reports/simple_report.pl.

Armen Gholian (S'12) received his Ph.D. degree in Electrical Engineering from the University of California, Riverside, CA, USA in 2015. Currently, he works at the instrument electronics development branch of National Aeronautics and Space Administration (NASA)'s Goddard Space Flight Center in Greenbelt, MD, USA. His research interests include wireless communications, digital signal processing, and optimization in smart grid.

Hamed Mohsenian-Rad (S'04-M'09-SM'14) received a Ph.D. degree in Electrical and Computer Engineering from the University of British Columbia in Vancouver, Canada in 2008, an M.Sc. degree in Electrical Engineering from Sharif University of Technology in 2004, and a B.Sc. degree in Electrical Engineering from Amir-Kabir University of Technology in 2002. Currently, he is an Assistant Professor of Electrical and Computer Engineering at the University of California at Riverside.

Dr. Mohsenian-Rad is the recipient of the National Science Foundation (NSF) CAREER Award 2012, the Best Paper Award from the IEEE Power and Energy Society General Meeting 2013, and the Best Paper Award from the IEEE International Conference on Smart Grid Communications 2012. He serves as Editor for the IEEE Trans. on Smart Grid, the IEEE Communications Surveys and Tutorials, and the IEEE Communications Letters. He has also served as the Symposium Co-chair of IEEE SmartGridComm'15 - Architectures, Control and Operation for Smart Grids and Microgrids Symposium, IEEE SmartGridComm'14 - Architectures, Control and Operation for Smart Grids and Microgrids Symposium, and IEEE SmartGridComm'13 - Demand Side Management, Demand Response, Dynamic Pricing Symposium. His research interests are the design, optimization, and game-theoretic analysis of power systems and electricity market.

Yingbo Hua (S'86-M'88-SM'92-F'02) received a B.S. degree (1982) from Southeast University, Nanjing, China, and a Ph.D. degree (1988) from Syracuse University, Syracuse, NY. He held a faculty position with the University of Melbourne in Australia during 1990-2000, where he was promoted to the rank of Reader and Associate Professor from 1996. After taking a leave as a visiting professor with Hong Kong University of Science and Technology in 1999-2000, and a consultant with Microsoft Research in summer 2000, he joined the University of California at Riverside in 2001, where he is a senior full professor.

Dr. Hua has served as Editor, Guest Editor, Member of Editorial Board and/or Member of Steering Committee for IEEE Transactions on Signal Processing, IEEE Signal Processing Letters, EURASIP Signal Processing, IEEE Signal Processing Magazine, IEEE Journal of Selected Areas in Communications, and IEEE Wireless Communication Letters. He has been a Member of IEEE Signal Processing Society's Technical Committees for Underwater Acoustic Signal Processing, Sensor Array and Multichannel Signal Processing, and Signal Processing for Communication and Networking. He has served on Technical and/or Organizing Committees for over fifty international conferences and workshops. He has authored/coauthored over three hundreds articles and coedited three volumes of books, with thousands of citations, in the fields of Sensing, Signal Processing and Communications. He is a Fellow of IEEE from 2002 and AAAS from 2011.